

The Spectrum of ^{12}C in a Multi-configuration Hartree-Fock Basis

K. Amos,^A I. Morrison,^A R. Smith^B and K. W. Schmid^{B,C}

^A School of Physics, University of Melbourne, Parkville, Vic. 3052.

^B Department of Theoretical Physics, Research School of Physical Sciences, Australian National University, P.O. Box 4, Canberra, A.C.T. 2600.

^C Permanent address: Institut für Theoretische-Physik, Universität Tübingen, West Germany.

Abstract

The energy level spectrum of ^{12}C is calculated in a truncated but large shell model space of projected one particle-one hole Hartree-Fock determinants using a realistic g matrix. Predictions of electromagnetic decays and electron scattering form factors are compared with experimental values.

1. Introduction

For many years the ^{12}C level spectrum has been a testing ground for theoretical models of nuclear structure ranging from the simplest TDA through RPA to sophisticated shell model studies (Gillet and Vinh Mau 1964; Cohen and Kurath 1965; Dehesa *et al.* 1977; Amos and Morrison 1979). Following the success of the shell model calculations (Cohen and Kurath 1965) in reproducing most of the then available experimental data, it was assumed that there was little left to learn about the ^{12}C system. But analyses of more recent scattering experiments ((p, p'), (π, π'), (e, e'), etc.) and measurements of electromagnetic decay rates (Flanz *et al.* 1979; Amos and Morrison 1979; Love 1980; Thiessen 1980; Ajzenberg-Selove and Busch 1980) require a re-evaluation either in terms of a refitted 0p-shell interaction or, as attempted herein, an *ab initio* calculation. The latter was chosen in view of the ever increasing empirical information in the energy region above 12 MeV the description of which is beyond the scope of the smaller basis 0p-shell models.

2. Particle-Hole Model (PHM)

Within the framework of standard Hartree-Fock (HF) theory (Villars 1963), an optimal reference determinantal wavefunction can be defined as

$$|\psi\rangle_A = \prod_{\alpha=1}^A b_{\alpha}^{\dagger} |\alpha\rangle, \quad (1)$$

where the (axially symmetric) deformed single particle states $|\alpha\rangle$ can be expanded in terms of oscillator basis states. Thus, with

$$|\alpha\rangle_{\Omega} = \sum_{nlj} C_{nlj,\alpha} |nlj\Omega\rangle, \quad (2)$$

the coefficients C_{α} are solutions of the HF equations. The reference determinant and the complete set of 1p-1h states (with respect to $|\psi\rangle_A$ and within the chosen oscillator basis) then define an intrinsic state basis for the PHM (Schmid 1980, 1981), from

which the nuclear eigenstates are obtained by diagonalizing the Hamiltonian of the system in a basis of physical states formed by angular momentum projection of these intrinsic states. This procedure limits spurious components in the resulting spectrum.

For $N \approx Z$ nuclei, the physical state vectors will then have the form, using the standard projection operators $\hat{P}(IMK)$ (MacDonald 1970),

$$|I^\pi MT; d\rangle = C_{0d}^{I^\pi 0} \{\hat{P}(I^+ M 0) |\psi_A\rangle\}_{T=0} + \sum_{\beta L} C_{\beta L; d}^{I^\pi T} \{\hat{P}(IMK_{L\beta}) b_\beta^\dagger b_L |\psi_A\rangle\}_T, \quad (3)$$

in which $\beta > F$ and $L \leq F$, the Fermi level. The eigenstates are then obtained (Watt 1971) by solving the non-orthogonal eigenvalue problem

$$(H_{KK}^{I^\pi T} - E^{I^\pi T} N_{KK}^{I^\pi T}) C^{I^\pi T} = 0, \quad (4)$$

in which the normalization (overlap) matrix N measures the lack of orthogonality of the projected intrinsic state vectors. The nuclear Hamiltonian, in standard form, is

$$H = \sum_{i=1}^A P_i^2/2m + \sum_{i < j} v_{ij}, \quad (5)$$

in which the v_{ij} are the Barrett-Hewitt-McCarthy two nucleon g matrices (Barrett *et al.* 1970, 1971). Centre of mass spuriousness in the eigenfunctions was minimized by a separate treatment of the centre of mass Hamiltonian.

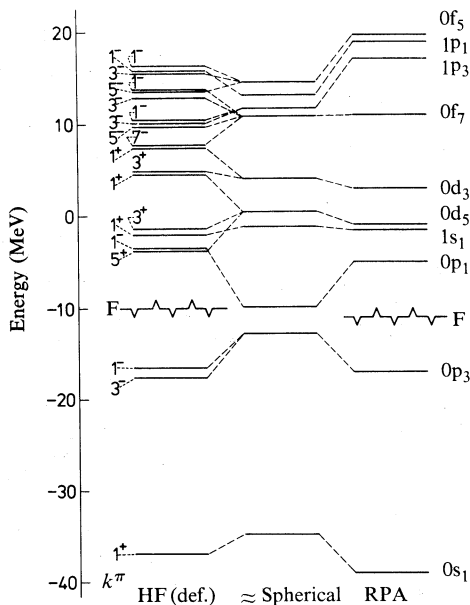


Fig. 1. Single particle spectrum for ^{12}C associated with the HF calculations (deformed field results classified by the k^π numbers shown to the left) compared with the equivalent spherical spectrum and the (spherical) RPA spectrum identified by the labels on the right. The Fermi levels are also shown.

Within the $0s_{1/2}$ to $0g_{9/2}$ inclusive spherical single particle basis (oscillator length of 1.79 fm), the minimal determinant for ^{12}C was then obtained by using starting energies $\hbar\omega$ that well predict (in HF studies) the single particle energies of ^{16}O and ^{40}Ca . By this means, the HF single particle spectrum, shown on the left in Fig. 1, was obtained. Good agreement up to about 10 MeV with the (spherical) single particle spectrum used in recent RPA calculations of ^{12}C (Dehesa *et al.* 1977) is

apparent by inspection of the two relevant results in Fig. 1. However, the underlying structure of the HF single particle states is contrary to the RPA assumption of $0p_{3/2}$ dominance as is evident in Table 1 where the expansion coefficients of the HF states as defined by equation (2) are given. Clearly, while the $0s_{1/2}$ and $0p_{3/2}$ states dominate the expansions of the $\frac{1}{2}^+$ and $\frac{3}{2}^-$ (k^π) states of the HF spectrum, the $\frac{1}{2}^-$ states are very strongly mixed. This is similar to Nilsson model calculations for open shell nuclei (Irvine 1972) and is largely independent of the character of the (realistic) g matrices, in so far as it is a self-consistent deformation field effect. Nevertheless, some changes in the degree of mixing are caused by the specific character of the g matrices, i.e. different central, tensor and spin-orbit components.

Table 1. HF single particle energies and wavefunctions in ^{12}C

k^π	ε (MeV)	$0s_{1/2}$	$1s_{1/2}$	$0d_{3/2}$	$0d_{5/2}$	$0g_{9/2}$	
$\frac{1}{2}^+$	-36.76	0.9751	0.1349	0.1206	-0.1279	0.0107	
$\frac{5}{2}^+$	-3.65				0.9977	-0.0681	
$\frac{1}{2}^+$	-1.98	-0.0534	0.8831	-0.0657	0.4584	-0.0545	
$\frac{3}{2}^+$	-1.31			0.6733	0.7355	-0.0755	
$\frac{1}{2}^+$	4.60	0.0907	-0.3643	0.5024	0.7722	-0.1020	
$\frac{3}{2}^+$	4.78			0.7394	-0.6687	0.0784	
$\frac{1}{2}^+$	7.71	-0.1952	0.2632	0.8537	-0.4008	0.0569	
$\frac{9}{2}^+$	21.53					1.0000	
$\frac{7}{2}^+$	23.24					1.0000	
$\frac{5}{2}^+$	24.46				0.0681	0.9977	
$\frac{3}{2}^+$	25.24			-0.0073	0.1086	0.9941	
$\frac{1}{2}^+$	25.62	0.0071	-0.0055	-0.0022	0.1290	0.9916	
		$0p_{1/2}$	$0p_{3/2}$	$1p_{1/2}$	$1p_{3/2}$	$0f_{5/2}$	$0f_{7/2}$
$\frac{3}{2}^-$	-17.64		0.9845		0.1128	0.0801	-0.0959
$\frac{1}{2}^-$	-16.48	0.7222	0.6701	0.0796	0.1061	-0.0599	-0.0901
$\frac{1}{2}^-$	-3.57	0.6710	-0.7189	-0.0040	0.0243	-0.1182	0.1356
$\frac{7}{2}^-$	7.75						1.0000
$\frac{5}{2}^-$	9.85					0.4592	0.8883
$\frac{3}{2}^-$	10.21		0.0709		-0.8532	-0.7537	-0.4933
$\frac{1}{2}^-$	10.57	0.0978	0.0233	-0.6233	-0.6898	-0.0980	-0.3405
$\frac{3}{2}^-$	12.83		0.1160		-0.5067	0.3056	0.7978
$\frac{5}{2}^-$	13.65					0.8883	-0.4592
$\frac{1}{2}^-$	13.74	0.0214	0.1685	-0.3919	-0.0937	0.1143	0.8920
$\frac{3}{2}^-$	15.62		0.1105		-0.0148	-0.9363	0.3332
$\frac{1}{2}^-$	15.67	-0.0100	0.0498	0.6534	-0.6730	-0.2461	0.2388
$\frac{1}{2}^-$	16.36	-0.1341	0.0522	-0.1569	0.2250	-0.9483	0.0695

The degree of mixing determines the equivalent spherical single particle spectrum via

$$\langle e_i \rangle = \sum_{\beta} e_{\beta} C_{i\beta}^2 \quad (6)$$

and these are shown in the centre section of Fig. 1. Clearly the effective (spherical) $0p$ -shell splitting is smaller (approximately 3 MeV) than used in usual calculations of spherical light nuclei (approximately 6 MeV for ^{16}O). The model thus will overestimate the $0p_{1/2}$ shell particle occupancy and this is revealed in Table 2 where the

occupancies are compared with those of a shell model (SM), an SU(3) (*LS* coupling) limit model, and the projected Hartree-Fock (PHFBA) model calculations (Smith *et al.* 1980). Clearly, the PHFBA and PHM occupancies are quite different to the SM values with the PHM being closest to the *LS* limit. This is a measure of the effective spin-orbit splitting and has important consequences in electron scattering analyses (Amos and Morrison 1979).

Table 2. Single particle occupancies in ^{12}C ground state

j	SM	SU(3)	PHFBA	PHM	j	SM	SU(3)	PHFBA	PHM
$0s_1$	2.00	2.00	1.94	1.90	$0d_5$	—	—	0.03	0.04
$0p_1$	0.74	1.33	0.96	1.04	$1p_1$	—	—	0.00	0.01
$0p_3$	3.27	2.67	2.99	2.84	$1p_3$	—	—	0.01	0.05
$1s_1$	—	—	0.01	0.04	$0f_5$	—	—	0.01	0.02
$0d_3$	—	—	0.02	0.03	$0f_7$	—	—	0.03	0.04

The PHM prediction of the ^{12}C energy spectrum is presented in Fig. 2 with the model energy levels being compared with the experimental values (Ajzenberg-Selove and Busch 1980). (For convenience they have been grouped by parity and isospin.) In making this comparison, we have not made any band head shift corrections (Schmid 1980, 1981) and it should be noted that the low excitation scale has been compressed by 3 MeV, whence the comparison of the 2_1^+ energy values is not as severe as could be thought. Indeed the 2_1^+ $T = 0$ state being too low by 1–1.5 MeV is quite common in such calculations (Caurier and Grammaticos 1977). Of the positive parity isoscalar states, the 0_2^+ state at 7.65 MeV excitation (and possibly the next two as well) is known to be dominantly a quartet excitation (4p–4h) with respect to the deformed ^{12}C ground state. As such it lies outside our model configuration space and therefore has no obvious theoretical counterpart in our spectrum, in contrast to the 1^+ and 4^+ states at 12.71 and 14.08 MeV excitation. Recent studies suggest other 1^+ isoscalar states in the region of 18 MeV excitation and of 2p–2h excitation. Mixtures of these excitations may be required to improve agreement between theoretical and experimental energies for the lowest 1^+ ($T=0$) state.

Given the above considerations, globally the predicted spectrum is in good agreement with experiment, especially since there are no free parameters in the interaction. In particular the parity and isospin band head energies are well predicted as are state sequences where empirical levels have been resolved.

We will be specifically interested hereafter with the 1^+ and 2^+ isovector states at 15.11 and 16.14 MeV excitation as these can be identified with wavefunctions of our PHM; albeit that we predict other and nearby isovector 1^+ and 2^+ states. These have not been seen empirically. Whilst no other states will be considered, we note the existence of a number of isoscalar and isovector 2^- , 3^- and 4^- states in the 17–20 MeV excitation region. These may have been observed in recent electron and pion inelastic scattering studies (Thiessen 1980). In view of the interest in these states in ^{16}O in the 18 MeV region vis-à-vis isospin mixing (Barker *et al.* 1981), further study of these states (and the reactions to them) in ^{12}C is planned.

From the calculated dipole states, the isoscalar and isovector E1 energy weighted sum rules were evaluated. The isoscalar component, which will vanish if the centre of mass spuriousness has been eliminated, was found to be only 2% of the isovector value.

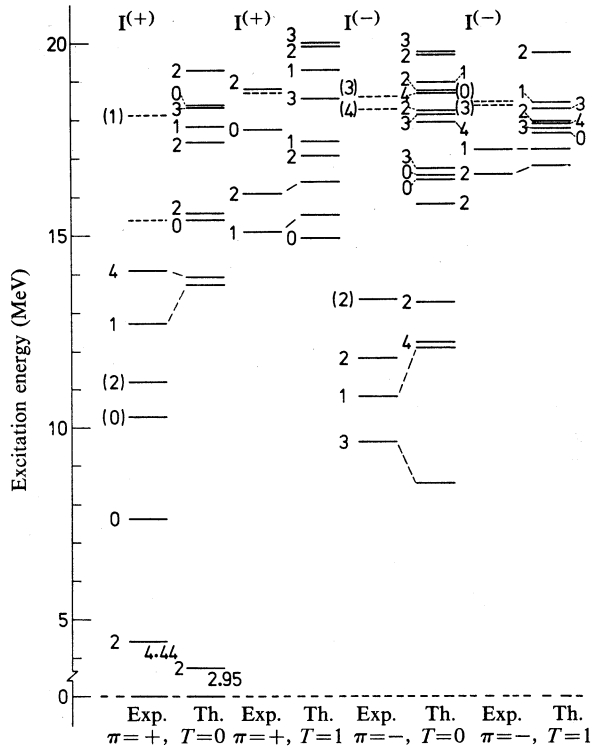


Fig. 2. ^{12}C energy spectrum resulting from the PHM calculations compared with the experimental values.

3. Transition Rates

Electromagnetic transition rates for the excitation of nuclei are predicted by evaluating reduced matrix elements of sums of the one body operators $t(i)$ between multinucleon states. The appropriate transition probabilities can be deduced to have the form (Nesci and Amos 1977)

$$B(XI; J_i \rightarrow J_f) = \{(2I+1)(2J_f+1)\}^{-1} \left(\sum_{j_1 j_2 \alpha} S_{j_1 j_2}^{(\alpha)} \langle \phi_{j_2} || t_\alpha(i) || \phi_{j_1} \rangle \right)^2, \quad (7)$$

in which the spectroscopic amplitudes, defined by

$$S_{j_1 j_2}^{(\alpha)} = \langle J_f(T_f) || [a_{j_2}^\dagger \times a_{j_1}]_{(\alpha)}^L || J_i(T_i) \rangle, \quad (8)$$

contain all the multinucleon structure information relevant to the transition. The same spectroscopic amplitudes are required in analyses of hadron inelastic scattering exciting the nuclear target state $|J_f(T_f)\rangle$ from the (ground) state $|J_i(T_i)\rangle$. For electromagnetic excitations, the one body operators have radial forms of the type r^L so that the single particle reduced matrix elements do not vary to any great extent with choice of bound state potential model, provided at least one relevant single particle state is bound by an MeV or more. Thus, variation in predictions of electromagnetic transition rates of low multipolarity should reflect dominantly the differences in the multinucleon spectroscopies chosen to specify the spectroscopic amplitudes.

With a study of ^{12}C transitions in mind, it is useful to define the spectroscopic amplitudes for a closed shell $(p_{3/2})^8$ model. For the 1^+ transitions,

$$S_{3/2\ 1/2}^{(\alpha)} = \left(\frac{3}{2}\right)^{\frac{1}{2}} \{ \delta_{\alpha-1/2} + (-)^T \delta_{\alpha 1/2} \} \quad (9)$$

are the only possible spectroscopic amplitudes if the 1^+ states are pure p-h states. The M1 transition probabilities are then given by

$$B(\text{M1}; 0^+ \rightarrow 1^+(T)) = \frac{1}{2} \{ \langle \phi_{1/2} || \text{M1}(p) || \phi_{3/2} \rangle + (-)^T \langle \phi_{1/2} || \text{M1}(n) || \phi_{3/2} \rangle \}^2. \quad (10)$$

Table 3. Spectroscopic amplitudes for excitation of $2^+(T=0)$ 4.44 MeV state in ^{12}C

j_1	j_2	SM	PHFBA	PHM	E2 element
0d ₃	0s ₁		0.114	0.170	2.65
0d ₅	0s ₁		0.128	0.184	3.24
0p ₃	0p ₁	1.195	1.086	0.935	3.42
1p ₃	0p ₁		0.054	0.141	-2.16
0f ₅	0p ₁		0.045	0.025	4.96
0p ₁	0p ₃	-0.704	-0.804	-0.845	-3.42
0p ₃	0p ₃	-0.503	-0.549	-0.654	-3.42
1p ₁	0p ₃			-0.095	2.16
1p ₃	0p ₃			-0.069	2.16
0f ₅	0p ₃			0.074	2.65
0f ₇	0p ₃		0.064	0.121	6.49
0d ₃	1s ₁			0.025	-4.33
0s ₁	0d ₃		-0.209	-0.203	-2.65
1s ₁	0d ₃			-0.028	-4.33
0s ₁	0d ₅		0.234	0.211	3.24
1s ₁	0d ₅			0.029	-5.30
0p ₃	1p ₁			0.097	-2.16
0p ₁	1p ₃			-0.131	2.16
0p ₃	1p ₃		-0.043	-0.055	2.16
0p ₁	0f ₅		0.056	0.101	4.96
0p ₃	0f ₅		-0.088	-0.108	-2.65
0p ₃	0f ₇		0.197	0.225	6.49
1p ₃	0f ₇			0.031	-8.21
$B(\text{E2})$		13.5	33.9	26.0	($e^2 \text{fm}^4$)

With the free particle g factors, this leads to predictions of 0.092 and $11.262 \mu_N^2$ (where μ_N is the nuclear magneton) for the isoscalar and isovector excitations respectively. The relevant experimental values are 0.045 ± 0.006 and $2.78 \pm 0.09 \mu_N^2$ (Ajzenberg-Selove and Busch 1980). Using the same model for E2 transitions, we find

$$B(\text{E2}; 0^+ \rightarrow 2^+) = \frac{1}{2} \{ e_p \langle \phi_{1/2} || \text{E2}(p) || \phi_{3/2} \rangle + (-)^T e_n \langle \phi_{1/2} || \text{E2}(n) || \phi_{3/2} \rangle \}^2 \quad (11)$$

from which, with bare charges, a value of $5.85 e^2 \text{fm}^4$ results for both the isovector and isoscalar transitions. Empirically, the 4.44 MeV isoscalar transition has a value of $38.8 \pm 2.2 e^2 \text{fm}^4$, whilst that of the 16.11 MeV isovector transition is $10.8 \pm 0.6 e^2 \text{fm}^4$; values that can be obtained provided proton (neutron) effective charges of $1.58e$ ($1.0e$) are used. While such large and dissimilar polarization charges as these

emphasize its limitations, this naive spectroscopic model provides base values in the jj coupling limit against which the results of more complex spectroscopies may be compared.

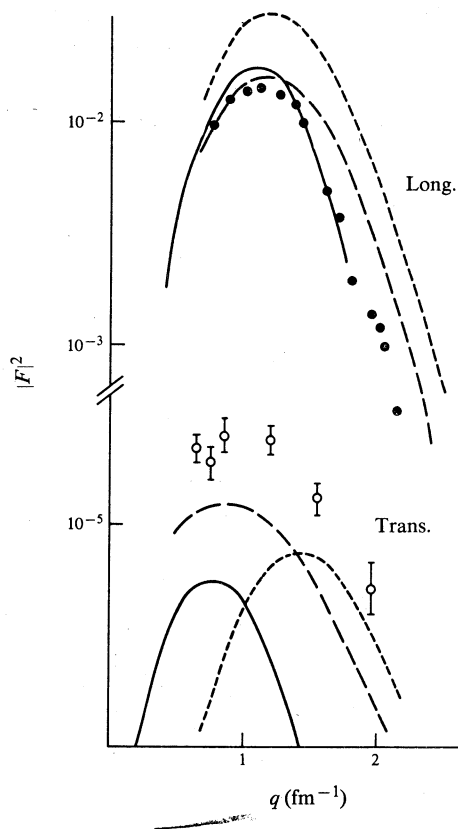


Fig. 3. Longitudinal and transverse (electric) form factors $|F|^2$ from inelastic electron scattering to the $2^+(T=0)$ 4.44 MeV state in ^{12}C . The solid curves give the PHM predictions whilst the long and short dash curves are the predictions obtained using the PHFBA and SM spectroscopy respectively (Amos and Morrison 1979).

The largest spectroscopic amplitudes in more complex models are given in Tables 3–5. Proton (and neutron) spectroscopic amplitudes for the excitation of the isoscalar 2^+ (4.44 MeV) state in ^{12}C are listed in Table 3 along with the results of 0p SM and the large basis PHFBA calculations (Amos and Morrison 1979). In addition the relevant single particle reduced E2 matrix elements are given in the last column from which the $B(E2)$ values listed were obtained. Two points emerge from this tabulation. First, while any non 0p-shell transition density is noticeably smaller than those within the 0p shell, their influence in $B(E2)$, (e, e') and (p, p') predictions (Amos and Morrison 1979) is significant. In such a ‘collective’ excitation all single particle contributions tend to add coherently. Such (isoscalar) $B(E2)$ values are therefore insensitive to distribution of the 0p-shell transition strengths through variations within the spectroscopic models. Second, the difference between the PHM and PHFBA results is primarily due to the destructive interference of the 0f–1p shell transition amplitudes in the PHM. Nevertheless, some physical attributes of the transition are sensitive to the relative contributions of the 0p-shell transitions in particular. The electron scattering transverse form factor is one such property being, as it is, sensitive to spin–orbit effects in the nuclear states. In particular, the magnetization (spin current)

contributions to transverse electric and magnetic form factors is maximized in the jj limit and vanishes identically in the LS (no spin-orbit) limit. This sensitivity is evident in Fig. 3 wherein the longitudinal and transverse form factors for the model calculations are compared with data (Flanz *et al.* 1979). Clearly the PHM (solid curves) and PHFBA model (large dash curves) predictions are similar in form for both the longitudinal and transverse form factors, notably in the peak momentum for the transverse form factor. The shape variations reflect our use of different oscillator lengths (1.79 fm for PHM, 1.7 fm for others). Clearly both HF based calculation results are distinct from the (small basis) SM results for the transverse form factor. The SM result for the longitudinal form factor, which includes a scaling correction

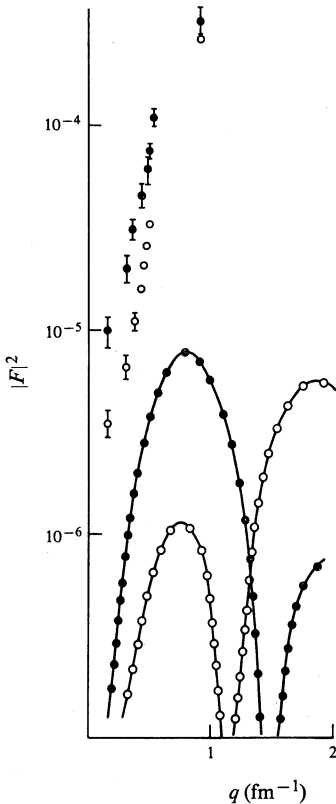


Fig. 4. Data and PHM predictions for the longitudinal (solid circles) and transverse (open circles) form factors for the isovector excitation by electron scattering of the 2^+ 16.11 ($T=1$) MeV state in ^{12}C .

for a polarization charge of $0.5e$, shows that an effective charge can account for any lack of coherence strength. This is not possible with the transverse form factor, however, since for momentum transfers greater than 1 fm^{-1} magnetization effects dominate form factor calculations (whence the PHM results, being nearest to the LS limit, are poorest), whilst for low momentum transfer values, the convection currents dominate and hence the failure of the small basis SM prediction. It appears, therefore, that a large basis HF calculation with the appropriate spin-orbit splitting may reproduce the data. The isospin and/or spin-flip transitions (specifically the $2_1^+(T=1)$, $1^+(T=0)$ and $1^+(T=1)$ states) are not 'collective' and are primarily determined by the $0\hbar\omega$ ($0p$ -shell) particle transitions. This is clearly the case for the

$2^+(T=1)$ transition when the PHM spectroscopic amplitudes given in Table 4 are considered. Further, if the single particle elements, also given in Table 4, are used to estimate the isovector $B(E2)$ value, strong cancellations occur and predictions then are very sensitive to details of the spectroscopy. As a consequence, our PHM calculation gave a value of $0.02 e^2 \text{fm}^4$ for this isovector $B(E2)$ value, whilst the naive model yielded a value of $5.85 e^2 \text{fm}^4$; a value also predicted by an RPA calculation (Friebel *et al.* 1978). The suppression of transition strength is further displayed in Fig. 4, wherein the predicted (PHM) longitudinal and transverse electric

Table 4. Proton spectroscopic amplitudes for excitation of $2^+(T=1)$ 16.11 MeV state in ^{12}C

j_1	j_2	S	E2 element	j_1	j_2	S	E2 element
0p ₃	0p ₁	-0.393	3.42	0f ₅	0p ₃	-0.012	2.65
1p ₃	0p ₁	-0.049	-2.16	0s ₁	0d ₅	0.012	3.24
0f ₅	0p ₁	-0.016	4.96	0p ₁	1p ₃	-0.014	2.16
0p ₁	0p ₃	0.354	-3.42	0p ₃	1p ₃	0.033	2.16
0p ₃	0p ₃	-0.725	-3.42	0p ₁	0f ₅	-0.028	4.96
1p ₁	0p ₃	-0.040	2.16	0p ₃	0f ₅	-0.039	-2.65
1p ₃	0p ₃	-0.093	2.16	0p ₃	0f ₇	-0.015	6.49

Table 5. Proton spectroscopic amplitudes for ^{12}C $1^+(T=0, 1)$ excitations

j_1	j_2	$T=0$		$T=1$		M1 elements	
		SM	PHM	SM	PHM	p	n
0p ₁	0p ₁	0.053	0.066	0.071	0.128	0.32	0.76
0p ₃	0p ₁	-0.880	-0.644	-0.845	-0.578	2.59	-2.16
1p ₁	0p ₁		0.007		-0.014		
1p ₃	0p ₁		-0.092		-0.084		
0p ₁	0p ₃	-0.434	-0.461	-0.416	-0.490	-2.59	2.16
0p ₃	0p ₃	-0.017	-0.027	-0.093	-0.167	4.78	-2.41
1p ₁	0p ₃		-0.052		-0.055		
1p ₃	0p ₃		-0.011		-0.032		
0f ₅	0p ₃		0.003		0.011		
0s ₁	1s ₁		0.023		0.016		
0s ₁	0d ₃		0.136		-0.047		
1s ₁	0d ₃		0.019		-0.006		
0p ₁	1p ₁		0.060		-0.020		
0p ₃	1p ₁		-0.010		-0.005		
0p ₁	1p ₃		-0.026		0.025		
0p ₃	1p ₃		0.008		0.031		
0p ₃	0f ₅		0.081		-0.027		
0p ₃	0f ₅		0.010		-0.004		
1f ₇	0f ₅		-0.004		-0.011	4.15	-3.46
$B(M1)$		0.014	0.004	2.77	0.77 (μ_N^2)		

electron scattering form factors for excitation of the isovector 2^+ state are compared with data. Clearly the almost complete cancellation amongst 0p-shell contributions from the PHM spectroscopy persists in the low q form factors. The SM calculations of Friebel *et al.* on the other hand gave quite good results.

The M1 excitation amplitudes for the $1^+(T=0)$ and $1^+(T=1)$ and relevant single particle matrix elements (now different for protons and neutrons because of differing g factors) are given in Table 5 where the PHM results are compared with the 0p SM

values. While it is evident that both transitions are dominated by the $0p$ -shell properties the different $0p_{3/2}$ shell ground state occupancies (see Table 2) give distinctly different values for the 1^+ spectroscopic amplitudes, and therefore for $B(M1)$ predictions. The $0p$ -shell components of the PHM amplitudes by themselves lead to $B(M1)$ values of 0.004 and $0.73 \mu_N^2$. For the isoscalar transition, it is the almost complete destructive interference between the $0p_{3/2} \rightarrow 0p_{1/2}$ and $0p_{1/2} \rightarrow 0p_{3/2}$ transitions that results in the small values, and while suppression of the isoscalar transition strength relative to the isovector is in accord with the experimental data, the suppres-

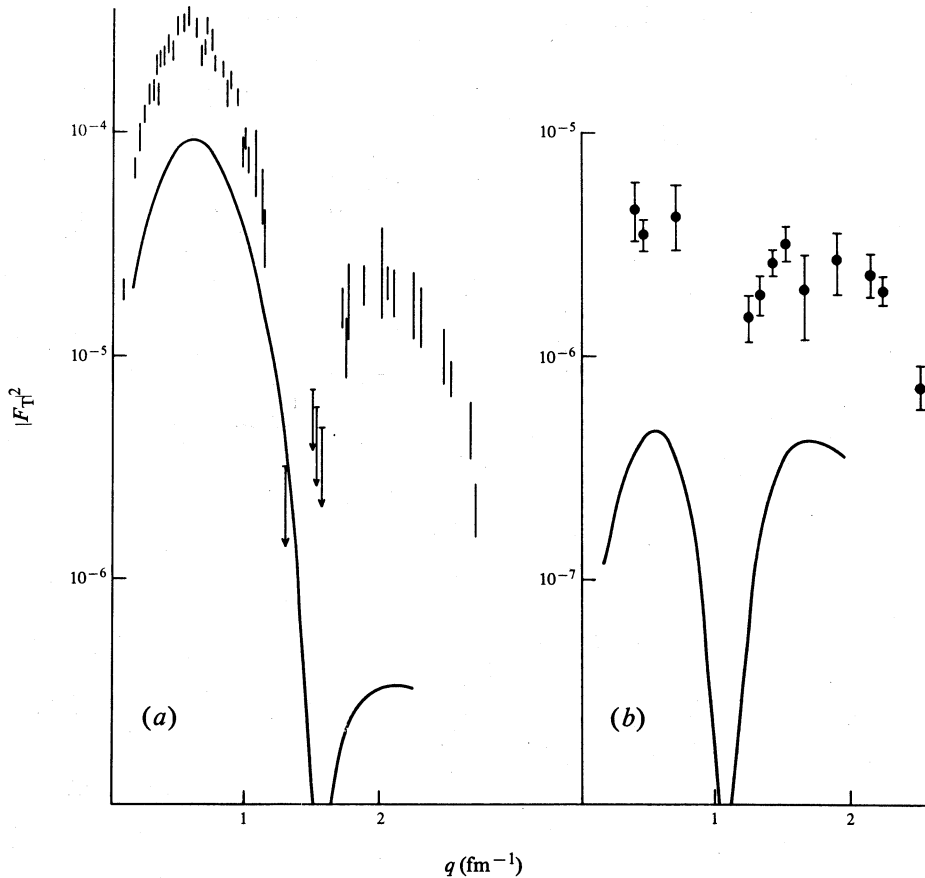


Fig. 5. Data and PHM predictions of the transverse form factors for the magnetic dipole excitations in ^{12}C for (a) the $1^+(T=1)$ 15.11 MeV state and (b) the $1^+(T=0)$ 12.71 MeV state.

sion is too complete, with the prediction being an order of magnitude below the experimental value ($0.045 \mu_N^2$). Clearly the simple SM result is much better, but even so it is still a factor of 3 weaker than experiment. Likewise for the isovector transition, strong cancellations yield too small a $B(M1)$ value from the PHM model, specifically $0.77 \mu_N^2$, which is to be compared with the $0p$ SM prediction of $2.77 \mu_N^2$, which in turn agrees well with the experimental value of $2.78 \mu_N^2$. In both the isoscalar and isovector transition cases, recalling that the naive spectroscopic model yielded $B(M1)$ values too large, model determinations of the magnetic dipole transition data are very

sensitive to the 0p-shell transition densities. Hadron scattering may also exhibit this sensitivity and the inability to date to fit data from the isoscalar excitation (Fox *et al.* 1979; Love 1980) may still be a spectroscopic rather than a reaction dynamics problem.

The marked suppression of magnetic dipole transition strength as predicted by the PHM spectroscopy is evident in Fig. 5 in which the isoscalar and isovector form factors are displayed. Whilst meson current corrections, for example, may significantly vary the larger q value predictions, clearly the PHM calculations give too much cancellation between the relevant matrix elements. These results are far removed from the good fits obtained in a previous SM calculation (Flanz *et al.* 1979). However in that study, the isovector transition data were fitted by adjusting the spectroscopic amplitudes and thus, by allowing isospin mixing to occur between the two 1^+ states, the good fit to the 12.71 MeV state data resulted. Clearly the sensitivity of $B(\text{M}1)$ values, and transverse form factors, to details of spectroscopy as we have demonstrated affords a good test of realistic (large basis) spectroscopic models of the ^{12}C system. In our present case, with the PHM approach, such tests reveal our inadequacy in the effective spherical spin-orbit field strength.

4. Conclusions

The PHM has been successful in generating a quantitative representation of the spectrum of ^{12}C up to ≈ 20 MeV excitation, for those states which can be classified as predominantly 1p-1h, using a fully microscopic, parameter free, Hamiltonian consisting of a two nucleon g matrix and one nucleon kinetic energies only. Electron scattering data and $B(\text{M}\lambda)$ rates to a few selected levels, however, show that the g matrix underestimates the effective spin-orbit splitting in the 0p shell. Due to the sensitivity of the spin-dependent data to small changes in the spin-orbit field, it should be possible to maintain the quality of the energy level spectrum whilst improving the electron scattering predictions. An investigation using other g matrices is in progress.

References

- Ajzenberg-Selove, F., and Busch, C. L. (1980). *Nucl. Phys. A* **336**, 1.
Amos, K., and Morrison, I. (1979). *Phys. Rev. C* **19**, 2108.
Barker, F., Smith, R., Morrison, I., and Amos, K. (1981). *J. Phys. G* **7**, 657.
Barrett, B. R., Hewitt, R. G. L., and McCarthy, R. J. (1970). *Phys. Rev. C* **2**, 1199.
Barrett, B. R., Hewitt, R. G. L., and McCarthy, R. J. (1971). *Phys. Rev. C* **3**, 1137.
Caurier, E., and Grammaticos, B. (1977). *Nucl. Phys. A* **279**, 333.
Cohen, S., and Kurath, D. (1965). *Nucl. Phys.* **73**, 1.
Dehesa, J. S., Krewald, S., Speth, J., and Faessler, A. (1977). *Phys. Rev. C* **15**, 1858.
Flanz, J. B., Hicks, R. S., Lindgren, R. A., Peterson, G. A., Dubach, J., and Haxton, W. C. (1979). *Phys. Rev. Lett.* **43**, 1922.
Fox, M., Morrison, I., Amos, K., and Weiss, D. (1979). *Phys. Lett. B* **86**, 121.
Friebel, A., Manakos, P., Richter, A., Spamer, E., Stock, W., and Titze, O. (1978). *Nucl. Phys. A* **294**, 129.
Gillet, V., and Vinh Mau, N. (1964). *Nucl. Phys.* **54**, 321.
Irvine, J. (1972). 'Nuclear Structure Theory' (Pergamon: Oxford).
Love, W. G. (1980). Proc. LAMPF Workshop on Nuclear Structure Studies with Intermediate Energy Probes, Los Alamos, New Mexico.
MacDonald, N. (1970). *Adv. Phys.* **19**, 371.
Nesci, P., and Amos, K. (1977). *Nucl. Phys. A* **284**, 239.

- Schmid, K. W. (1980). *An. Fis.* **76**, 63.
- Schmid, K. W. (1981). *Phys. Rev.* (in press).
- Smith, R., Morrison, I., and Amos, K. (1980). *Aust. J. Phys.* **33**, 1.
- Thiessen, H. A. (1980). *Nucl. Phys. A* **335**, 329.
- Villars, F. (1963). Proc. Int. School of Physics 'Enrico Fermi', Course XXIII, p. 1 (Academic: New York).
- Watt, A. (1971). *Nucl. Phys. A* **172**, 260.

Manuscript received 6 April 1981, accepted 12 June 1981